ELSEVIER

Kaon production and kaon to pion ratio in Au + Au collisions at $\sqrt{s_{NN}} = 130$ GeV

STAR Collaboration

C. Adler [k], Z. Ahammed [w], C. Allgower [l], J. Amonett [n], B.D. Anderson [n], M. Anderson [e],
G.S. Averichev [i], J. Balewski [l], O. Barannikova [i,w], L.S. Barnby [n], J. Baudot [m],
S. Bekele [t], V.V. Belaga [i], R. Bellwied [ae], J. Berger [k], H. Bichsel [ad], A. Billmeier [ae],
L.C. Bland [b], C.O. Blyth [c], B.E. Bonner [x], A. Boucham [z], A. Brandin [r], A. Bravar [b],
R.V. Cadman [a], H. Caines [t], M. Calderón de la Barca Sánchez [b], A. Cardenas [w],
J. Carroll [o], J. Castillo [z], M. Castro [ae], D. Cebra [e], P. Chaloupka [t], S. Chattopadhyay [ae],
Y. Chen [f], S.P. Chernenko [i], M. Cherney [h], A. Chikanian [ag], B. Choi [ab], W. Christie [b],
J.P. Coffin [m], T.M. Cormier [ae], J.G. Cramer [ad], H.J. Crawford [d], W.S. Deng [b],
A.A. Derevschikov [v], L. Didenko [b], T. Dietel [k], J.E. Draper [e], V.B. Dunin [i],
J.C. Dunlop [ag], V. Eckardt [p], L.G. Efimov [i], V. Emelianov [r], J. Engelage [d], G. Eppley [x],
B. Erazmus [z], P. Fachini [b], V. Faine [b], K. Filimonov [o], E. Finch [ag], Y. Fisyak [b], D. Flierl [k],
K.J. Foley [b], J. Fu [o,af], C.A. Gagliardi [aa], N. Gagunashvili [i], J. Gans [ag], L. Gaudichet [z],
M. Germain [m], F. Geurts [x], V. Ghazikhanian [f], O. Grachov [ae], V. Grigoriev [r],
M. Guedon [m], E. Gushin [r], T.J. Hallman [b], D. Hardtke [o], J.W. Harris [ag], T.W. Henry [aa],
S. Heppelmann [u], T. Herston [w], B. Hippolyte [m], A. Hirsch [w], E. Hjort [o],
G.W. Hoffmann [ab], M. Horsley [ag], H.Z. Huang [f], T.J. Humanic [t], G. Igo [f], A. Ishihara [ab],
Yu.I. Ivanshin [j], P. Jacobs [o], W.W. Jacobs [l], M. Janik [ac], I. Johnson [o], P.G. Jones [c],
E.G. Judd [d], M. Kaneta [o], M. Kaplan [g], D. Keane [n], J. Kiryluk [f], A. Kisiel [ac], J. Klay [o],
S.R. Klein [o], A. Klyachko [l], A.S. Konstantinov [v], M. Kopytine [n], L. Kotchenda [r],
A.D. Kovalenko [i], M. Kramer [s], P. Kravtsov [r], K. Krueger [a], C. Kuhn [m], A.I. Kulikov [i],
G.J. Kunde [ag], C.L. Kunz [g], R.Kh. Kutuev [j], A.A. Kuznetsov [i], L. Lakehal-Ayat [z],
M.A.C. Lamont [c], J.M. Landgraf [b], S. Lange [k], C.P. Lansdell [ab], B. Lasiuk [ag], F. Laue [b],
A. Lebedev [b], R. Lednický [i], V.M. Leontiev [v], M.J. LeVine [b], Q. Li [ae], S.J. Lindenbaum [s],
M.A. Lisa [t], F. Liu [af], L. Liu [af], Z. Liu [af], Q.J. Liu [ad], T. Ljubicic [b], W.J. Llope [x],
G. LoCurto [p], H. Long [f], R.S. Longacre [b], M. Lopez-Noriega [t], W.A. Love [b], T. Ludlam [b],
D. Lynn [b], J. Ma [f], R. Majka [ag], S. Margetis [n], C. Markert [ag], L. Martin [z], J. Marx [o],
H.S. Matis [o], Yu.A. Matulenko [v], T.S. McShane [h], F. Meissner [o], Yu. Melnick [v],
A. Meschanin [v], M. Messer [b], M.L. Miller [ag], Z. Milosevich [g], N.G. Minaev [v],

J. Mitchell [x], V.A. Moiseenko [j], C.F. Moore [ab], V. Morozov [o], M.M. de Moura [ae],
M.G. Munhoz [y], J.M. Nelson [c], P. Nevski [b], V.A. Nikitin [j], L.V. Nogach [v], B. Norman [n],
S.B. Nurushev [v], G. Odyniec [o], A. Ogawa [u], V. Okorokov [r], M. Oldenburg [p], D. Olson [o],
G. Paic [t], S.U. Pandey [ae], Y. Panebratsev [i], S.Y. Panitkin [b], A.I. Pavlinov [ae], T. Pawlak [ac],
V. Perevoztchikov [b], W. Peryt [ac], V.A. Petrov [j], M. Planinic [l], J. Pluta [ac], N. Porile [w],
J. Porter [b], A.M. Poskanzer [o], E. Potrebenikova [i], D. Prindle [ad], C. Pruneau [ae],
J. Putschke [p], G. Rai [o], G. Rakness [l], O. Ravel [z], R.L. Ray [ab], S.V. Razin [i,l],
D. Reichhold [h], J.G. Reid [ad], F. Retiere [o], A. Ridiger [r], H.G. Ritter [o], J.B. Roberts [x],
O.V. Rogachevski [i], J.L. Romero [e], A. Rose [ae], C. Roy [z], V. Rykov [ae], I. Sakrejda [o],
S. Salur [ag], J. Sandweiss [ag], A.C. Saulys [b], I. Savin [j], J. Schambach [ab], R.P. Scharenberg [w],
N. Schmitz [p], L.S. Schroeder [o], A. Schüttauf [p], K. Schweda [o], J. Seger [h], D. Seliverstov [r],
P. Seyboth [p], E. Shahaliev [i], K.E. Shestermanov [v], S.S. Shimanskii [i], V.S. Shvetcov [j],
G. Skoro [i], N. Smirnov [ag], R. Snellings [o], P. Sorensen [f], J. Sowinski [l], H.M. Spinka [a],
B. Srivastava [w], E.J. Stephenson [l], R. Stock [k], A. Stolpovsky [ae], M. Strikhanov [r],
B. Stringfellow [w], C. Struck [k], A.A.P. Suaide [ae], E. Sugarbaker [t], C. Suire [b],
M. Šumbera [t], B. Surrow [b], T.J.M. Symons [o], A. Szanto de Toledo [y], P. Szarwas [ac],
A. Tai [f], J. Takahashi [y], A.H. Tang [n], J.H. Thomas [o], M. Thompson [c], V. Tikhomirov [r],
M. Tokarev [i], M.B. Tonjes [q], T.A. Trainor [ad], S. Trentalange [f], R.E. Tribble [aa],
V. Trofimov [r], O. Tsai [f], T. Ullrich [b], D.G. Underwood [a], G. Van Buren [b],
A.M. VanderMolen [q], I.M. Vasilevski [j], A.N. Vasiliev [v], S.E. Vigdor [l], S.A. Voloshin [ae],
F. Wang [w], H. Ward [ab], J.W. Watson [n], R. Wells [t], G.D. Westfall [q], C. Whitten Jr. [f],
H. Wieman [o], R. Willson [t], S.W. Wissink [l], R. Witt [ag], J. Wood [f], N. Xu [o], Z. Xu [b],
A.E. Yakutin [v], E. Yamamoto [o], J. Yang [f], P. Yepes [x], V.I. Yurevich [i], Y.V. Zanevski [i],
I. Zborovský [i], H. Zhang [ag], W.M. Zhang [n], R. Zoulkarneev [j], A.N. Zubarev [i]

[a] *Argonne National Laboratory, Argonne, IL 60439, USA*
[b] *Brookhaven National Laboratory, Upton, NY 11973, USA*
[c] *University of Birmingham, Birmingham, United Kingdom*
[d] *University of California, Berkeley, CA 94720, USA*
[e] *University of California, Davis, CA 95616, USA*
[f] *University of California, Los Angeles, CA 90095, USA*
[g] *Carnegie Mellon University, Pittsburgh, PA 15213, USA*
[h] *Creighton University, Omaha, NE 68178, USA*
[i] *Laboratory for High Energy (JINR), Dubna, Russia*
[j] *Particle Physics Laboratory (JINR), Dubna, Russia*
[k] *University of Frankfurt, Frankfurt, Germany*
[l] *Indiana University, Bloomington, IN 47408, USA*
[m] *Institut de Recherches Subatomiques, Strasbourg, France*
[n] *Kent State University, Kent, OH 44242, USA*
[o] *Lawrence Berkeley National Laboratory, Berkeley, CA 94720, USA*
[p] *Max-Planck-Institut fuer Physik, Munich, Germany*
[q] *Michigan State University, East Lansing, MI 48824, USA*
[r] *Moscow Engineering Physics Institute, Moscow, Russia*
[s] *City College of New York, New York City, NY 10031, USA*
[t] *Ohio State University, Columbus, OH 43210, USA*

[u] *Pennsylvania State University, University Park, PA 16802, USA*
[v] *Institute of High Energy Physics, Protvino, Russia*
[w] *Purdue University, West Lafayette, IN 47907, USA*
[x] *Rice University, Houston, TX 77251, USA*
[y] *Universidade de Sao Paulo, Sao Paulo, Brazil*
[z] *SUBATECH, Nantes, France*
[aa] *Texas A&M University, College Station, TX 77843, USA*
[ab] *University of Texas, Austin, TX 78712, USA*
[ac] *Warsaw University of Technology, Warsaw, Poland*
[ad] *University of Washington, Seattle, WA 98195, USA*
[ae] *Wayne State University, Detroit, MI 48201, USA*
[af] *Institute of Particle Physics, CCNU (HZNU), Wuhan, 430079 China*
[ag] *Yale University, New Haven, CT 06520, USA*

Abstract

Mid-rapidity transverse mass spectra and multiplicity densities of charged and neutral kaons are reported for Au + Au collisions at $\sqrt{s_{NN}} = 130$ GeV at RHIC. The spectra are exponential in transverse mass, with an inverse slope of about 280 MeV in central collisions. The multiplicity densities for these particles scale with the negative hadron pseudo-rapidity density. The charged kaon to pion ratios are $K^+/\pi^- = 0.161 \pm 0.002(\text{stat}) \pm 0.024(\text{syst})$ and $K^-/\pi^- = 0.146 \pm 0.002(\text{stat}) \pm 0.022(\text{syst})$ for the most central collisions. The K^+/π^- ratio is lower than the same ratio observed at the SPS while the K^-/π^- is higher than the SPS result. The ratios are enhanced by about 50% relative to p + p and p̄ + p collision data at similar energies.
© 2004 Elsevier B.V. Open access under CC BY license.

PACS: 25.75.-q; 25.75.Dw

Lattice QCD predicts that at sufficiently high energy density, accessible in relativistic heavy-ion collisions, matter will be in a state of deconfined quarks and gluons [1]. It has been suggested that strangeness production is a sensitive probe of a deconfined state: for example, strangeness production may be enhanced by the fast and energetically favorable process of gluon–gluon fusion into strange quark–antiquark pairs [2]. Hadronic mechanisms, on the other hand, may also enhance strangeness production [3]. A systematic investigation of strangeness production may therefore provide crucial input for understanding the matter created in heavy-ion collisions.

Strangeness production has been studied in heavy-ion collisions at the AGS [4–6], SPS [7–10], and more recently at RHIC [11–13]. In this Letter, we report measurements by the STAR experiment at RHIC on charged and neutral kaon production. The measurements were made at mid-rapidity in Au + Au collisions at a nucleon–nucleon center-of-mass energy of $\sqrt{s_{NN}} = 130$ GeV. The measurements were carried out during the summer of 2000 and details of the STAR experiment are described elsewhere [14–16]. The primary tracking device in the experiment is a Time Projection Chamber (TPC). It sits in a magnetic field of 0.25 Tesla. Tracks were reconstructed from three-dimensional hits measured in the TPC and the primary vertex of the interaction was found by fitting the reconstructed tracks to a common point of origin. Corrections were made for the energy loss of the charged kaons in the detector material.

Two methods were used to identify the kaons:

(I) The energy loss method (dE/dx). Particle identification was done by measuring the mean specific energy lost by the charged particles, $\langle dE/dx \rangle$, in the

E-mail address: fqwang@physics.purdue.edu (F. Wang).

TPC gas. The $\langle dE/dx \rangle$ resolution was approximately 11%. The tracks were required to come from within 3 cm of the primary vertex and every track had at least 25 hits, out of 45 possible hits, on the TPC pad plane. Using a method that is described in [16], the distribution in $\ln[\langle dE/dx \rangle/\langle dE/dx \rangle_{BB}]$ (where $\langle dE/dx \rangle_{BB}$ is the expected Bethe–Bloch value) was fit by a sum of four Gaussians corresponding to $\pi^{\pm}$, $K^{\pm}$, $e^{\pm}$, and p ($\bar{p}$). The fit was done for each centrality and transverse momentum ($p_{\perp}$) bin. The raw kaon yield was extracted from the fit parameters. The kaon rapidity was limited to $|y| < 0.1$. In the range where the kaons are well separated from other species, $p_{\perp} \lesssim 0.5$ GeV/c, we estimate a point-to-point systematic error of 5% on the extracted kaon yields. In the range where the kaons and the $e^{\pm}$ overlap in $\langle dE/dx \rangle$, $0.5 \lesssim p_{\perp} \lesssim 0.7$ GeV/c, we parameterized the $e^{\pm}$ yield using data from lower $p_{\perp}$ and Monte Carlo (MC) simulations and estimate the systematic errors to range from 10% to 20%. In the region where the kaons significantly merge with the pions in $\langle dE/dx \rangle$, $0.7 \lesssim p_{\perp} \lesssim 0.8$ GeV/c, we neglect the $e^{\pm}$ contribution and estimate the systematic errors to be on the order of 15% [17].

(II) The Decay topology method (*Kink* and K_S^0). Charged kaons can be identified topologically via their one-prong, 'kink', decays (e.g., $K \rightarrow \mu\nu$, $K \rightarrow \pi\pi^0$) [18,19]. The parent kaon and charged daughter tracks are used to determine the decay kinematics. Kaons with rapidity $|y| < 0.5$ were used in the analysis. To improve the signal to background ratio and allow for adequate daughter momentum measurement, the decay position was restricted by a fiducial cut inside the volume of the TPC. Background sources include charged pion decays, hadronic interactions in the TPC gas, and combinatorics. A momentum dependent decay angle cut was used to eliminate essentially all pion decays because they have a much smaller decay angle. A remaining background of the order of 15% is corrected for in the kaon spectra. About 70% of this is combinatorial background, and the rest is mainly hadronic interactions. Details of the analysis can be found in [19].

Neutral kaons were reconstructed via their decay $K_S^0 \rightarrow \pi^+\pi^-$. A pair of oppositely charged tracks formed a K_S^0 decay-candidate if their distance of closest approach to each other was less than 1 cm. The majority of the combinatorial background was eliminated by requiring that the daughter tracks miss the primary vertex by at least 1.5 cm, and the decay vertex had to be separated from the primary vertex by more than 6 cm [20]. A cut on the $\langle dE/dx \rangle$ of the daughters was also applied to remove the majority of the contribution from $\Lambda \rightarrow p\pi^-$ and $\bar{\Lambda} \rightarrow \bar{p}\pi^+$ decays. After these cuts the signal to background ratio ranges from 5 to 12 as evaluated at the peak position of the invariant mass distribution. The remaining background is well described by a third order polynomial in the region of the K_S^0 mass and was subtracted from the $\pi^+\pi^-$ invariant mass distribution to obtain the raw K_S^0 yield. K_S^0 with rapidity $|y| < 0.5$ were used in the analysis.

In all cases, the primary vertex was restricted to a limited longitudinal range near the center of the TPC. The event centrality was determined off-line and is based on measured charged particle multiplicities in the TPC. A correction factor was applied to account for losses due to limited acceptance, decay, tracking inefficiency, and hadronic interactions. The overall efficiency (ϵ), including all these effects, was obtained from a full MC simulation by embedding MC tracks into real events on the raw data level. For the most central collisions, the dE/dx method yielded $\epsilon \simeq$ 20% at $p_{\perp} = 0.2$ GeV/c and 60% at 0.7 GeV/c. For the *Kink* method, $\epsilon \simeq 1.5\%$ at $p_{\perp} = 1$ GeV/c and 0.6% at 2 GeV/c. For the K_S^0 method, $\epsilon \simeq 4.5\%$ at $p_{\perp} = 1$ GeV/c and 7% at 2 GeV/c. The efficiency increases with decreasing event multiplicity by about 20% of its value, from the most central to the most peripheral bins, for the dE/dx and *Kink* methods and by 70% for the K_S^0 method. Momentum resolution was estimated to be 2% for dE/dx identified kaons at $p_{\perp} = 0.5$ GeV/c and 3% for *Kink* and 2–4% for K_S^0, respectively, over the measured $p_{\perp}$ range. The momentum resolution was found to have negligible effect on the kaon spectra and so no correction was applied.

Fig. 1 shows the transverse mass spectra for the invariant yields of K^+, K^-, and K_S^0, where $m_{\perp} \equiv \sqrt{(p_{\perp}^2 + m^2)^{1/2}}$ and m is the kaon mass. The errors shown for the dE/dx method are the quadratic sum of the statistical and point-to-point systematic errors. The errors shown for *Kink* and K_S^0 methods are statistical only. The systematic errors on the spectra are estimated by varying event and track selections, track
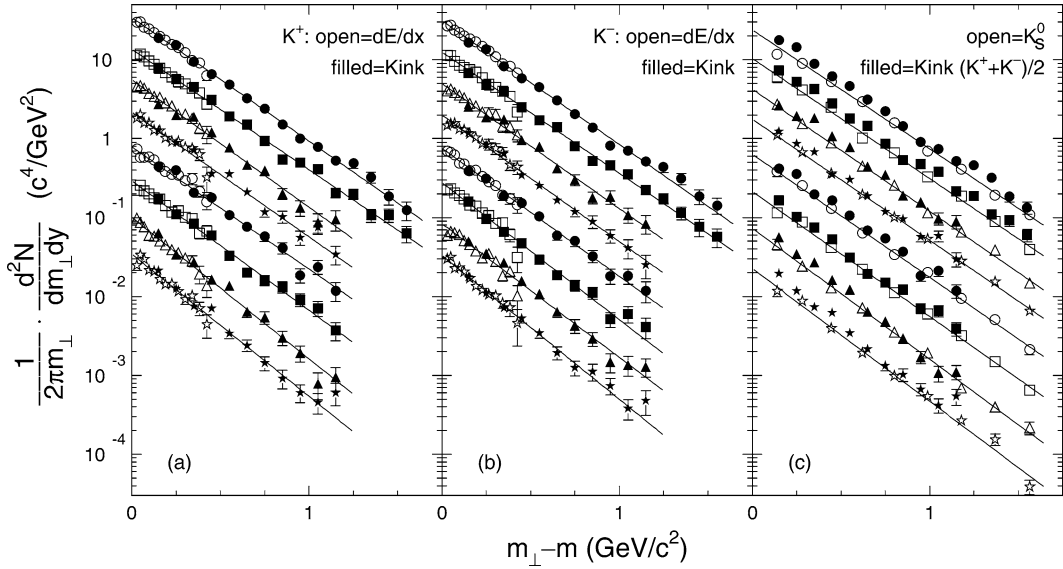
Fig. 1. Invariant yields for K^+, K^- and K_S^0 versus $m_\perp$. In figure (a) K^+ and (b) K^-, the kaons are identified by the dE/dx method ($|y| < 0.1$) and by the *Kink* method ($|y| < 0.5$). In figure (c) the K_S^0 is identified by the K_S^0 method ($|y| < 0.5$) and the $(K^+ + K^-)/2$ is from the *Kink* analysis. The data are plotted in order of decreasing centrality from top to bottom. See Table 2. The most central collision spectrum is shown full scale; the other spectra are divided by 2, 4, 8, 16, 32, 64, and 64 for display purposes. The error bars are uncorrelated random errors. See text and Table 1 for a description of the systematic errors. The solid lines are $m_\perp$ exponential fits to the K^+, K^-, and K_S^0 spectra, respectively.

Table 1
Summary of systematic errors correlated within each method. Those marked as "separate" are not correlated between different methods, while those marked as "common" are correlated

	dE/dx	*Kink*	K_S^0
On spectra (separate)	5%	10%	10%
On spectra (common)	5%	5%	5%
	Charged kaons		K_S^0
On dN/dy (separate)	8%		10%
On dN/dy (common)	5%		5%
On T (separate)	8%		8%

quality cuts, and other analysis cuts. The estimated systematic errors are 5%, 10%, and 10% for dE/dx, *Kink*, and K_S^0 methods, respectively. They are uncorrelated among the three analyses. An additional 5% systematic error, due to uncertainties in our MC determination of the efficiencies, applies to all three analyses. The systematic errors are listed in Table 1. Fig. 1(c) compares K_S^0 spectra to the averaged charged kaon spectra from the *Kink* method. The kaon spectra exhibit an exponential shape in $m_\perp$. We fit the spectra of charged kaons (combined from dE/dx and *Kink*)

and K_S^0, respectively, to an $m_\perp$ exponential with the inverse slope, T, and the integrated rapidity density, dN/dy, as free parameters. The fit results are shown as solid lines in Fig. 1. The fit parameters are listed in Table 2 together with $dN_{h^-}/d\eta$, the negative hadron multiplicity within $|\eta| < 0.5$ [15]. Systematic errors on dN/dy and T are both about 8% for charged kaons, and 10% and 8%, respectively, for K_S^0 (see Table 1). The systematic errors are partially correlated between K^+ and K^-. An additional 5% systematic error applies to the dN/dy and it is correlated between all three particle species.

Our charged kaon dN/dy results are in agreement with the recent PHENIX publication [12] and the point-by-point spectra agree within two standard deviations of systematic errors. The difference in our measured dN/dy between K_S^0 and the average of charged kaons is 1–2.5 standard deviations of systematic errors. As isospin asymmetry is negligible at midrapidity [21], the primordial K_S^0 yield is most likely equal to the average of the primordial charged kaon yields. Our measurements include decay products of ϕ mesons which decay into charged kaons and neutral kaons with different branching ratios. However, the ef-

Table 2

The mid-rapidity kaon multiplicity densities (dN/dy) and $m_\perp$ exponential inverse slopes (T in MeV) as a function of negative hadron multiplicity within $|\eta| < 0.5$ ($dN_{h^-}/d\eta$). Quoted errors are uncorrelated errors (first) and correlated systematic errors (second). See text and Table 1 for details. Systematic error on $dN_{h^-}/d\eta$ is 7%. The centrality bins are as same as in Ref. [16]

| Centrality bin	$dN_{h^-}/d\eta$	K^+		K^-		K_S^0	
		dN/dy	T	dN/dy	T	dN/dy	T
58–85%	17.9	$2.46 \pm 0.07 \pm 0.32$	$241 \pm 7 \pm 19$	$2.32 \pm 0.06 \pm 0.30$	$238 \pm 7 \pm 19$	$1.76 \pm 0.09 \pm 0.26$	$258 \pm 7 \pm 21$
45–58%	47.3	$7.23 \pm 0.18 \pm 0.94$	$242 \pm 6 \pm 19$	$6.48 \pm 0.17 \pm 0.84$	$257 \pm 7 \pm 21$	$5.83 \pm 0.26 \pm 0.87$	$262 \pm 6 \pm 21$
34–45%	78.9	$11.8 \pm 0.3 \pm 1.5$	$265 \pm 6 \pm 21$	$10.4 \pm 0.2 \pm 1.4$	$250 \pm 6 \pm 20$	$9.07 \pm 0.34 \pm 1.36$	$275 \pm 6 \pm 22$
26–34%	115.0	$17.2 \pm 0.4 \pm 2.2$	$281 \pm 7 \pm 22$	$15.5 \pm 0.4 \pm 2.0$	$268 \pm 7 \pm 21$	$13.7 \pm 0.5 \pm 2.1$	$279 \pm 6 \pm 22$
18–26%	154.0	$23.1 \pm 0.5 \pm 3.0$	$275 \pm 7 \pm 22$	$20.8 \pm 0.5 \pm 2.7$	$271 \pm 7 \pm 22$	$19.5 \pm 0.7 \pm 2.9$	$283 \pm 6 \pm 23$
11–18%	196.0	$28.8 \pm 0.7 \pm 3.7$	$269 \pm 6 \pm 22$	$26.4 \pm 0.6 \pm 3.4$	$274 \pm 7 \pm 22$	$23.1 \pm 0.8 \pm 3.5$	$280 \pm 6 \pm 22$
6–11%	236.0	$38.0 \pm 0.6 \pm 4.9$	$284 \pm 4 \pm 23$	$34.5 \pm 0.5 \pm 4.5$	$283 \pm 4 \pm 23$	$29.0 \pm 1.2 \pm 4.3$	$285 \pm 6 \pm 23$
0–6%	290.0	$46.2 \pm 0.6 \pm 6.0$	$277 \pm 4 \pm 22$	$41.9 \pm 0.6 \pm 5.4$	$277 \pm 4 \pm 22$	$33.9 \pm 1.1 \pm 5.1$	$288 \pm 5 \pm 23$
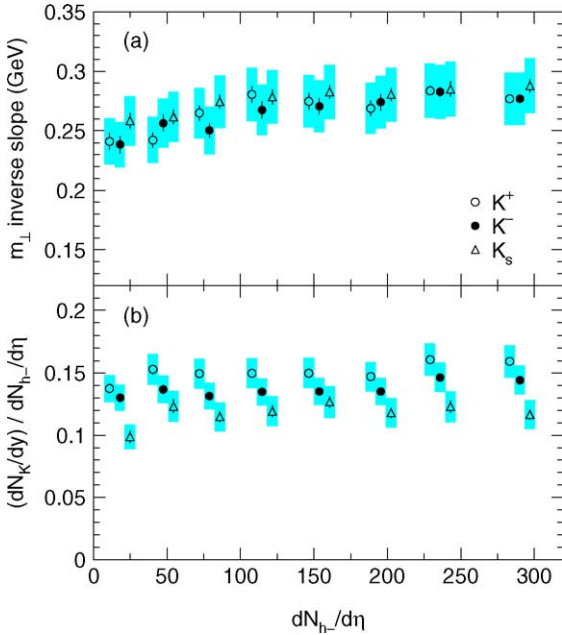
Fig. 2. The centrality dependence of (a) kaon inverse slopes and (b) mid-rapidity kaon to negative hadron ratios. The error bars are uncorrelated random errors; correlated systematic errors are indicated by the shaded areas. An additional systematic error (not shown) of 5% and 7% applies to the dN/dy of kaons and $dN_{h^-}/d\eta$, respectively. For clarity the K^+ and K_S^0 points are displaced in $dN_{h^-}/d\eta$.

fect is estimated, using the measured ϕ spectra [11], to be less than 3%.

Fig. 2(a) shows T as a function of $dN_{h^-}/d\eta$. No difference is observed between the K^+, K^- and K_S^0. There is an indication of a systematic increase in T

from ~ 240 MeV in the most peripheral collisions to ~ 280 MeV in the most central collisions. For comparison, the kaon inverse slope is about 240 MeV for central heavy-ion collisions at the SPS ($\sqrt{s_{NN}} \approx 17$ GeV) [8,9,22] and 200 MeV at the AGS ($\sqrt{s_{NN}} \approx 5$ GeV) [5,6]. Note, however, that inverse slopes may measure a combined effect of thermal temperature and transverse radial flow [22] and the larger T values suggest stronger radial flow at RHIC energies. For the most central collisions, the measured kaon T is smaller than that of the lambda and the lambda dN/dy [13] is about 1/3 of the kaon dN/dy. As a result, the lambda yield approaches and exceeds the kaon yield at $p_\perp \sim 1.5$ GeV/c. At larger $p_\perp$ perturbative hard-scattering phenomena become important [12,23]. A similar behaviour was also observed for non-strange particles (pion and proton) [12].

Fig. 2(b) shows the ratio of kaon dN/dy to $dN_{h^-}/d\eta$ as a function of $dN_{h^-}/d\eta$. No strong centrality dependence is observed for the ratios, suggesting no significant change in strangeness production mechanisms from peripheral to central collisions at this RHIC energy.

K/π ratios are often used to study strangeness production enhancement. In order to evaluate K/π, we deduce the mid-rapidity pion dN_{π^-}/dy in central collisions from our measurements of negative hadrons [15], antiprotons [16] and K^- spectra. The deduced mid-rapidity value is $dN_{\pi^-}/dy = 287 \pm 20$ (syst + stat), consistent with STAR preliminary measurement of pion spectra [24]. For the most central collisions, $K^+/\pi^- = 0.161 \pm 0.002(\text{stat}) \pm 0.024(\text{syst})$ and $K^-/\pi^- = 0.146 \pm 0.002(\text{stat}) \pm 0.022(\text{syst})$. The
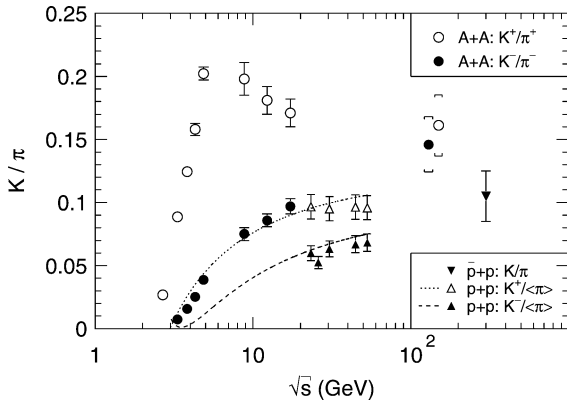
Fig. 3. Mid-rapidity K/π ratios versus $\sqrt{s_{NN}}$. The curves are parameterizations to p + p data [28]. The error bars show statistical errors. The systematic errors on the STAR data are indicated by the caps. The STAR K^+/π point is displaced in $\sqrt{s_{NN}}$ for clarity.

systematic errors are a quadratic sum of those on the kaon and the pion dN/dy. Fig. 3 is a compilation of K/π results for central heavy-ion collisions. Since mid-rapidity $\pi^+/\pi^- \approx 1$ at RHIC [21], we can readily compare our K^+/π^- results to K^+/π^+ results from lower energies. The K^-/π ratio steadily increases with $\sqrt{s_{NN}}$, while the K^+/π ratio in heavy-ion collisions sharply increases at low energies and the maximum value of K^+/π^+ occurs at $\sqrt{s_{NN}} \sim 10$ GeV. This value is determined by the interplay between dropping of the net-baryon density with $\sqrt{s_{NN}}$ and increasing of the $K\bar{K}$ pair production rate, as previously noted (e.g., in [25–27]).

Fig. 3 also shows parameterized p + p data (curves) and data from p + p [28] and $\bar{p}$ + p [29] at high energies. The average of π^+ and π^- multiplicities, $\langle\pi\rangle$, is used to form the ratios in order to take into account the isospin effect. Our measurement indicates an enhancement in the K/π ratios of about 50% in central Au + Au collisions over the elementary collisions extrapolated to similar energies. The origin of the enhancement needs further studies as the interpretation requires detailed and systematic modeling. For example, within the RQMD model the K/π ratio is sensitive to particle rescattering but insensitive to the formation of phenomenological color ropes [26].

A similar magnitude of enhancement in K^-/π has been already observed at the lower energies of the AGS [5] and SPS [8]. The enhancement in K^+/π is even larger at lower energies due to the larger net-

baryon density. At lower energies the enhancement increases gradually as the collisions become more central, roughly doubling from peripheral to central collisions. In contrast, the enhancement at RHIC remains unchanged from the measured peripheral to central collisions. Since the K/π ratios are sensitive to chemical freeze-out conditions, this behavior implies that these conditions change from peripheral to central collisions at the AGS and SPS, but not at RHIC. Since the initial conditions are likely different over the measured centrality range, the observed independence of the K/π ratios on centrality at chemical freeze-out is interesting and needs further investigation.

In conclusion, we have reported invariant yield transverse mass spectra and multiplicity densities of charged and neutral kaons at mid-rapidity in Au + Au collisions at $\sqrt{s_{NN}} = 130$ GeV at RHIC. The spectra are described by an exponential in transverse mass. The inverse slope parameters are found to increase slightly with collision centrality, with a value of about 280 MeV in central collisions. No strong centrality dependence is found in the ratio of kaon rapidity densities to negative hadron pseudo-rapidity densities, in contrast to results from low energies at the AGS and SPS. For the most central collisions, the mid-rapidity kaon to pion ratios are $K^+/\pi^- = 0.161 \pm 0.002(\text{stat}) \pm 0.024(\text{syst})$ and $K^-/\pi^- = 0.146 \pm 0.002(\text{stat}) \pm 0.022(\text{syst})$. For central heavy ion collisions, the K^+/π ratio is found to increase rapidly with the collision energy and then to decrease, while the K^-/π ratio increases steadily. This behavior is consistent with the increasing pair production rate as the collision energy increases, and the decreasing net-baryon density at mid-rapidity. The measured K/π ratios at RHIC show an enhancement of about 50% over p + p and $\bar{p}$ + p collisions at similar energies.

References

[1] E. Laermann, Nucl. Phys. A 610 (1996) 1c.

[2] J. Rafelski, B. Müller, Phys. Rev. Lett. 48 (1982) 1066;
J. Rafelski, B. Müller, Phys. Rev. Lett. 56 (1986) 2334, Erratum;
J. Rafelski, Phys. Rep. 88 (1982) 331;
R. Koch, B. Müller, J. Rafelski, Phys. Rep. 142 (1986) 167.

[3] H. Sorge, et al., Phys. Lett. B 271 (1991) 37;
H. Sorge, Phys. Rev. C 52 (1995) 3291.

[4] E802 Collaboration, T. Abbott, et al., Phys. Rev. Lett. 66 (1991) 1567;
T. Abbott, et al., Phys. Rev. D 45 (1992) 3906;
T. Abbott, et al., Phys. Rev. C 50 (1994) 1024.

[5] E802 Collaboration, L. Ahle, et al., Phys. Rev. C 60 (1999) 044904;
L. Ahle, et al., Phys. Rev. C 58 (1998) 3523;
L. Ahle, et al., Phys. Rev. C 57 (1998) 466;
E802 Collaboration, F. Wang, et al., in: Proc. of Heavy-Ion Physics at the AGS, 1996, WSU-NP-96-16.

[6] E866 Collaboration, L. Ahle, et al., E917 Collaboration, B.B. Back, et al., Phys. Lett. B 476 (2000) 1;
E866 Collaboration, L. Ahle, et al., E917 Collaboration, B.B. Back, et al., Phys. Lett. B 490 (2000) 53.

[7] NA35 Collaboration, J. Bartke, et al., Z. Phys. C 48 (1990) 191;
T. Alber, et al., Eur. Phys. J. C 2 (1998) 643.

[8] NA49 Collaboration, F. Siklér, et al., Nucl. Phys. A 661 (1999) 45c;
C. Höhne, Nucl. Phys. A 661 (1999) 485c;
S.V. Afanasiev, et al., Phys. Rev. C 66 (2002) 054902.

[9] NA44 Collaboration, I.G. Bearden, et al., Phys. Lett. B 471 (1999) 6;
H. Bøggild, et al., Phys. Rev. C 59 (1999) 328;
I.G. Bearden, et al., Phys. Rev. C 66 (2002) 044907.

[10] WA97 Collaboration, E. Andersen, et al., Phys. Lett. B 449 (1999) 401.

[11] STAR Collaboration, C. Adler, et al., Phys. Rev. C 65 (2002) 041901R.

[12] PHENIX Collaboration, K. Adcox, et al., Phys. Rev. Lett. 88 (2002) 242301.

[13] STAR Collaboration, C. Adler, et al., Phys. Rev. Lett. 89 (2002) 092301.

[14] STAR Collaboration, K.H. Ackermann, et al., Nucl. Phys. A 661 (1999) 681c;
C. Adler, et al., Phys. Rev. Lett. 86 (2001) 4778.

[15] STAR Collaboration, C. Adler, et al., Phys. Rev. Lett. 87 (2001) 112303.

[16] STAR Collaboration, C. Adler, et al., Phys. Rev. Lett. 87 (2001) 262302.

[17] A. Cardenas, Ph.D. Thesis, Purdue University, 2002.

[18] S. Margetis, K. Safarik, O. Villalobos Baillie, Annu. Rev. Nucl. Part. Sci. 50 (2000) 299.

[19] W. Deng, Ph.D. Thesis, Kent State University, 2002, http://cnr2.kent.edu/~margetis/theses/w_deng/thesis.

[20] M.A.C. Lamont, Ph.D. Thesis, University of Birmingham, 2002.

[21] PHOBOS Collaboration, B.B. Back, et al., Phys. Rev. Lett. 87 (2001) 102301.

[22] NA44 Collaboration, I.G. Bearden, et al., Phys. Rev. Lett. 78 (1997) 2080;
N. Xu, M. Kaneta, Nucl. Phys. A 698 (2002) 306c.

[23] STAR Collaboration, J. Adams, et al., Phys. Rev. Lett. 92 (2004) 52302.

[24] STAR Collaboration, J.W. Harris, Nucl. Phys. A 698 (2002) 64c;
M. Calderón de la Barca Sánchez, Ph.D. Thesis, Yale University, 2001, nucl-ex/0111004.

[25] F. Wang, Phys. Lett. B 489 (2000) 273.

[26] F. Wang, et al., Phys. Rev. C 61 (2000) 064904.

[27] F. Wang, N. Xu, Phys. Rev. C. 61 (2000) 021904;
J.C. Dunlop, C.A. Ogilvie, Phys. Rev. C 61 (2000) 031901;
P. Braun-Munzinger, et al., Nucl. Phys. A 697 (2002) 902.

[28] A.M. Rossi, et al., Nucl. Phys. B 84 (1975) 269;
NA23 Collaboration, J.L. Bailly, et al., Phys. Lett. B 195 (1987) 609.

[29] T. Alexopoulos, et al., Phys. Rev. D 48 (1993) 984.